Available online at www.sciencedirect.com
ScienceDirect
Estuarine, Coastal and Shelf Science 71 (2007) 250–258
ESTUARINE COASTAL AND SHELF SCIENCE
www.elsevier.com/locate/ecss

Relative availability of satellite imagery and ship-based sampling for assessment of stormwater runoff plumes in coastal southern California

Nikolay P. Nezlin*, Stephen B. Weisberg, Dario W. Diehl

Southern California Coastal Water Research Project, 7171 Fenwick Lane, Westminster, CA 92683-5218, USA

Received 23 March 2006; accepted 27 July 2006
Available online 8 September 2006

Abstract

Information about the size and intensity of urban runoff plumes in the ocean has traditionally been collected through ship-based surveys, but sampling from ships in the nearshore zone is weather-dependent because of the rough sea conditions that often accompany storms. High-resolution satellite imagery is an alternative approach for assessing plume properties, but the availability of satellite imagery can also be weather-dependent. Here we compare the logistical availability of ship-based sampling and the quality of satellite imagery for assessing rainstorm-mediated freshwater plumes. The availability of ship-based sampling was assessed by correlating deployment success of three local ships with wind and wave data and then applying those relationships to a longer wind and wave data record. The quality of satellite imagery was assessed by correlating cloud cover and expert opinion about the usefulness of Level 2 SeaWiFS imagery, then analyzing those relationships with respect to cloud cover found in Level 3 AVHRR, SeaWiFS, and MODIS imagery. In the 10 days following storm events, ships were found to be capable of deployment for sampling about 70% of the time, while SeaWiFS produced high quality images only about 23% of the time. The days for which satellite imagery and ship-based data were available often differed, yielding complementary, rather than redundant, information. As a result, plume data were available for about 80% of the study period using one of the methods. The probability of obtaining usable satellite imagery was lowest on the day of a rainstorm and increased during the next 5 days, whereas the probability of obtaining ship-based data was highest on the day of the storm and typically declined in the days following a storm. MODIS sensors provided better coverage than SeaWiFS or AVHRR due to better spectral, spatial, and particularly temporal resolution (twice a day), thereby significantly improving information about plume dynamics.

Keywords: coastal waters; plumes; satellite sensing; monitoring; USA, southern California

1. Introduction

Stormwater runoff is a major source of contaminants to the southern California coastal ocean (Ackerman and Weisberg, 2003; Bay et al., 2003; Noble et al., 2003; Schiff and Bay, 2003; Reeves et al., 2004). After strong rainstorms, optical signatures of freshwater plumes have been observed as far as 30 km offshore (Warrick et al., 2004a; Ahn et al., 2005; Nezlin and DiGiacomo, 2005). The size of these plumes is affected by natural factors such as rainfall volume and intensity (Nezlin et al., 2005), but effective management (e.g., issuance of swimmer health warnings after storms) requires an understanding of how plume size and concentration of pollutants in the plumes are also affected by anthropogenic factors such as land use practices.

Traditionally, information about the size and intensity of plumes has been collected through ship-based surveys. However, samples in the nearshore zone are typically collected from vessels that are sensitive to sea state, especially high-speed wind and wind-driven short-period waves. Such conditions typically occur during and immediately after a rainstorm, when the plume data are most critical.

Satellite imagery offers an alternative approach for assessing plume properties. Ocean color is correlated with important plume characteristics, such as salinity (Monahan and Pybus,

* Corresponding author.
E-mail address: nikolayn@sccwrp.org (N.P. Nezlin).

0272-7714/$ - see front matter © 2006 Elsevier Ltd. All rights reserved.
doi:10.1016/j.ecss.2006.07.016

1978; Vasilkov et al., 1999; Siddorn et al., 2001) and suspended matter (Mertes et al., 1998; Sathyendranath, 2000; Mertes and Warrick, 2001; Toole and Siegel, 2001; Otero and Siegel, 2004; Warrick et al., 2004b). Satellite imagery is less expensive to obtain than ship-based measurements, because environmental data from government-operated satellites are freely available. Also, satellite imagery provides a more synoptic assessment than can be achieved by a slow moving ship trying to capture a rapidly evolving stormwater plume.

The availability of useful satellite imagery, though, can also be weather-dependent. The most valuable satellite data are ocean color and infrared satellite imagery, but the quality of this imagery depends on atmospheric transparency, which can be compromised by clouds that are often present during and shortly after a storm. Moreover, the best such imagery is from near-polar sun-synchronous satellites, which typically pass over an area only once per day during daylight hours, compounding concerns about satellite view angle, the transparency of the atmosphere, etc. Present-day geostationary satellites (e.g., GOES) provide more frequent data, but the higher altitude and lower resolution of these satellites limit the value of their data for near coastal assessments. Freshwater discharge plumes can also be detected using weather-independent synthetic aperture radar (SAR) to assess sea surface roughness (Svejkovsky and Jones, 2001; DiGiacomo et al., 2004), but SAR is more expensive, employs fewer satellite overpasses and provides a less direct measure of plumes than visible imagery.

Here we compare the relative logistical efficacy and potential synergy of ship-based sampling and imagery from polar orbiting satellites used as tools for describing rainstorm-mediated freshwater plumes. In particular, we compare the availability of ship-based sampling data (ocean conditions calm enough for ships to leave port) with the availability of acceptable (not overly-obscured by cloud cover) satellite imagery for the 10 days following rainstorms on southern California's continental shelf.

2. Methods

2.1. Satellite imagery

We examined image quality for four types of satellite data: (1) Sea-viewing Wide Field-of-view Sensor (SeaWiFS) Level 2 normalized water-leaving radiation of 555-nm wavelength; (2) SeaWiFS Level 3 chlorophyll; (3) Advanced Very High Resolution Radiometer (AVHRR) Level 3 Sea Surface Temperature (SST); and (4) Moderate-Resolution Imaging Spectroradiometer (MODIS) Level 3 SST.

The first data type was obtained using the SeaWiFS, an ocean color radiometer that measures the electromagnetic radiation reflected by the ocean surface at 8 wavebands from 412 to 865 nm (McClain et al., 2004). These data were evaluated by providing imagery for the 10 days following every rainstorm between 19 and 21 UTM (i.e., 11–13 local time) to four water quality experts (three are authors of this paper) and asking them to rate each image from 0 (no image) to 5 (a perfect image) with respect to information obtained about plume pattern (Table 1). The ratings provided by the experts were then averaged and classified into three groups: "Bad" (mean rating <2.5, indicating that there was little usable information obtained), "Moderate" (mean rating 2.5–3.5, indicating that some information was obtained, but not enough to observe the entire plume), and "Good" (mean rating >3.5, indicating that the plume could be reasonably well observed).

The images provided to the experts were normalized water-leaving radiation of 555-nm wavelength, which was selected because this optical property is a good proxy for freshwater plumes after rainstorms (Otero and Siegel, 2004; Nezlin and DiGiacomo, 2005; Nezlin et al., 2005). The images were generated as measured radiance counts (Level 1 data), processed to geophysical characteristics of the ocean surface (i.e., Level 2 data) using the conventional SeaDAS algorithm.

The other three image types were evaluated by quantifying cloud cover from the images and scoring them based on the correlation between cloud cover and the expert ratings that were determined from the Level 2 SeaWiFS images. One of these was Level 3 SeaWiFS chlorophyll data. We used Level 3 files for the period September 1997–December 2004 obtained from the Goddard Space Flight Center Distributed Active Archive Center (GSFC DAAC).

AVHRR (Cracknell, 1997) cloud cover was quantified with Level 3 Pathfinder V5 SST images for the period January 1997–December 2004 obtained from the Jet Propulsion Laboratory Physical Oceanography Distributed Active Archive Center (JPL PODAAC). These data include quality codes (QC) for cloud contamination with values from 0 to 7 assigned to each pixel (7 = best quality). We selected SST images with QCs from 4 to 7 for analysis, and defined pixels with QCs from 0 to 3 as "missing data".

The fourth satellite data type was from MODIS, a visible/infrared sensor onboard two NASA satellites: *Terra* and *Aqua*. We used MODIS Level 3 SST data produced at NASA by the algorithm similar to AVHRR Pathfinder (Kilpatrick et al., 2001). The data were obtained from JPL in the format similar to Pathfinder V5 SST. The data records started from October 2000 (MODIS-Terra) and November 2002 (MODIS-Aqua) and ended in December 2004. Quality codes from 0 (best quality) to 3 (worst quality) were used to characterize each pixel; the study utilized pixels with QC = 0.

Table 1
Criteria used for rating the quality of SeaWiFS satellite images

Rank	Description
0	No image due to complete cloud cover or absence of satellite pass
1	Either a small ocean area is visible through clouds or the resolution is dramatically decreased due to low satellite view angle
2	A significant part of ocean area is cloud-free, but the plume zone is obscured
3	Some information on plume pattern (or plume absence) can be recognized
4	Plume pattern (or plume absence) is evident
5	Perfect image

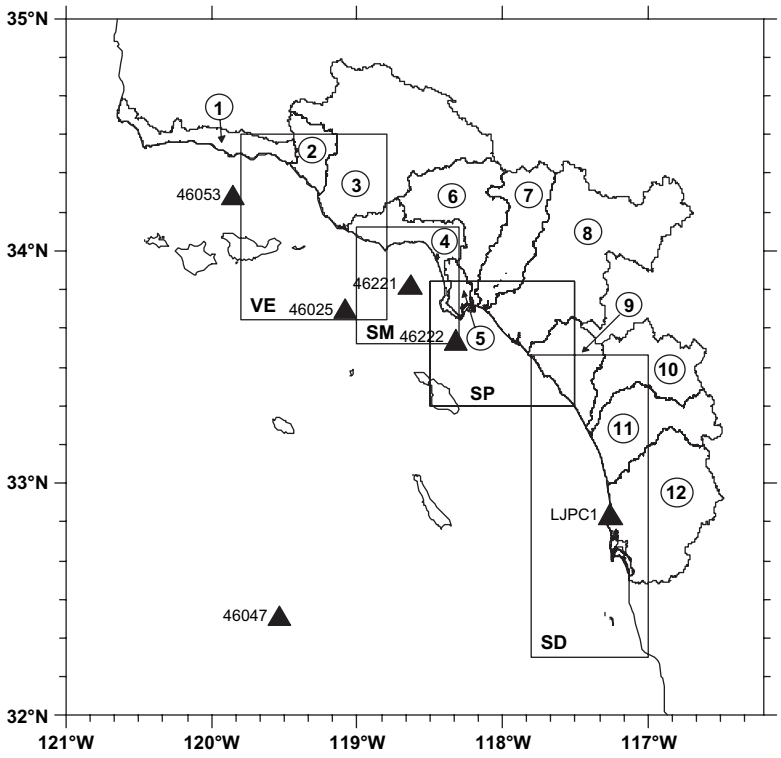

Fig. 1. The four regions for which the availability of satellite data was analyzed: VE – Ventura; SM – Santa Monica Bay; SP – San Pedro Shelf; SD – Orange County/San Diego. The numerals in circles indicate the coastal watersheds where the rainstorm magnitude was estimated. Black triangles indicate buoys where wind and wave data were measured.

For each type of satellite data, separate estimates of imagery quality were made for four regions corresponding to the major watersheds draining into the Southern California Bight (SCB) (Fig. 1, Table 2). A rainstorm was defined as beginning when accumulated precipitation exceeded 2.54 cm after a 7-day period when precipitation did not exceed this threshold. Using this definition, there were 35 rainstorms in Ventura, 30 in Santa Monica, 29 in San Pedro, and 29 in San Diego region between 1997 and 2004. Rainstorm events in the southern California coastal watersheds were evaluated using precipitation data obtained from the 185 rain-gauge stations in central and southern California through the National Climatic Data Center (http://cdo.ncdc.noaa.gov/CDO/cdo). Since all rain-gauge stations did not contain complete records of

Table 2
Four regions of southern California analyzed for quality of satellite images after rainstorms

Region	Ocean		Land	
	Latitude	Longitude	Watersheds	Area (km^2)
1. Ventura	33.70°N–34.50°N	119.8°W–118.8°W	Santa Barbara Creek	971
			Ventura River	696
			Santa Clara River	5164
			Ventura region (total)	6831
2. Santa Monica Bay	33.60°N–34.10°N	119.0°W–118.3°W	Malibu Creek	286
			Ballona Creek	338
			Santa Monica Bay region (total)	1170
3. San Pedro Shelf	33.33°N–33.87°N	118.5°W–117.5°W	Dominguez Channel	300
			Los Angeles River	2161
			San Gabriel River	1758
			Santa Ana River	5101
			San Pedro Shelf region (total)	9320
4. Orange County/San Diego	32.25°N–33.55°N	117.8°W–117.0°W	San Juan Creek	1284
			Santa Margarita River	1915
			San Luis Rey River/Escondido Creek	2002
			San Diego River	3561
			Orange County/San Diego region (total)	8762

Table 3
The buoys used for the analysis of wind and wave conditions

NDBC identifier	Latitude	Longitude	Water depth (m)	Parameters
1. 46053	34° 14.17 N	119° 51.00 W	417.0	Wind vector (04/1998–12/2004)
				Wave height (04/1998–12/2004)
2. 46221	33° 51.27 N	118° 37.96 W	363.0	Wave height and direction (01/1997–12/2004)
3. 46025	33° 44.70 N	119° 05.03 W	859.5	Wind vector (01/1997–12/2004)
				Wave height (01/1997–12/2004)
4. 46222	33° 37.07 N	118° 19.02 W	457.0	Wave height and direction (02/1998–12/2004)
5. LJPC1	32° 52.00 N	117° 15.40 W	7.0	Wind vector (01/1997–11/2004)
				Wave height (01/1997–12/2004)
6. 46047	32° 26.00 N	119° 31.98 W	1393.5	Wind vector (05/1999–12/2004)
				Wave height (05/1999–12/2004)

observations, available rain-gauge data were fitted to unified periods (i.e., calendar days) and interpolated using kriging (Isaaks and Srivastava, 1989). Precipitation was then integrated over each of the four study regions and divided by the region area to obtain mean precipitation for each day.

2.2. Ship-based data

The availability of ships for assessing runoff plumes was evaluated by examining the logs from three southern California ships that have been used to sample plumes, correlating their deployment success with wind and wave conditions, and then applying these relationships to more extensive records of oceanographic conditions. The three ships were the R/V *La Mer* (85 ft. located in Santa Monica Bay), the R/V *Monitor III* (42 ft. located in San Diego) and the R/V *Metro* (30 ft. located in San Diego). Logbooks for these ships were available from 1998 to 2004 during which they cumulatively weathered out 61 times.

Wind speed and wave height data were obtained for six buoys (Fig. 1; Table 3) from the National Data Buoy Center (http://www.ndbc.noaa.gov). Absolute wave height (m) was measured at all six buoys; wave direction at two buoys, and wind speed ($m\,s^{-1}$) and direction at four buoys (Table 3). Absolute values for wave height and wind speed were averaged over 3-h time intervals and analyzed for each rainstorm event, from 5 days prior, until 10 days afterward.

To define the meteorological conditions influencing ship deployment, we calculated the mean and standard deviation for wind speed and wave height on days when vessels were weathered out (Table 4). We then classified the likelihood of successful deployment into three categories: ''Good'' (neither wind speed nor wave height exceeded the mean from Table 4), ''Moderate'' (either wind speed or wave height exceeded the mean, but did not exceed the mean plus standard deviation), and ''Bad'' (either wind speed or wave height exceeded the mean plus a standard deviation).

3. Results

3.1. Satellite imagery

The ratings for quality of the SeaWiFS Level 2 imagery provided by the four experts were highly correlated ($r = 0.89–0.94$). The experts determined that 63% of the images across all regions and days provided no information about plume dynamics. Only 23% of the images contained enough information to reasonably identify size and shape of the plume, while the remainder contained some visible pixels but not enough to be of value to managers. The best quality imagery was for the Ventura area and the poorest was for Orange County/San Diego area (Table 5). The quality of SeaWiFS imagery was lowest on the day of a storm, when less than 10% of the images in all regions were of good quality (Fig. 2). However, this percentage more than doubled to an average of approximately 25% for the 2 days following a storm.

The spatial and temporal patterns of imagery quality were similar for SeaWiFS, AVHRR and MODIS (Fig. 3). However, the quality of MODIS images was consistently better than that of SeaWiFS, with AVHRR images consistently exhibiting the lowest quality. All sensors recorded less than 10% of cloud-free area on the day of a storm, but MODIS images recorded

Table 4
Statistical characteristics of wind speed and wave height for the periods from 8 UTC to 24 UTC (midnight to 16:00 local time) during the days when boat trips were weathered out

NDBC buoy	Boat	Wind speed ($m\,s^{-1}$)				Wave height (m)			
		Mean	SD	Mean − SD	Mean + SD	Mean	SD	Mean − SD	Mean + SD
46053	*La Mer*	7.6616	3.5926	4.0690	11.2542	2.2048	0.7555	1.4493	2.9603
46221		–	–	–	–	1.9651	0.6226	1.3425	2.5877
46025		8.6673	3.0636	5.6037	11.7309	2.3445	0.7045	1.6400	3.0490
46222		–	–	–	–	1.8141	0.5658	1.2483	2.3799
LJPC1	*Monitor III/Metro*	4.6068	1.9478	2.6590	6.5546	1.4008	0.5680	0.8328	1.9688
46047		10.4856	3.3227	7.1629	13.8083	3.6969	1.2704	2.4265	4.9673

Table 5
Probability of conditions being favorable for boat sampling or for obtaining informative satellite images in different areas of the Southern California Bight averaged for the 10 days starting from the day of rainstorm

Region	Boat	Buoy	Conditions for boat sampling		
			Good (%)	Moderate (%)	Bad (%)
Santa Monica Bay	*La Mer*	46025	75.3	15.1	9.6
San Diego	*Monitor III*, *Metro*	LJPC1	74.6	18.5	6.9

Region	SeaWiFS satellite imagery		
	Good (3.5–5) (%)	Moderate (2.5–3.5) (%)	Bad (0–2.5) (%)
Ventura	28.8	8.7	62.5
Santa Monica	29.6	9.6	60.8
San Pedro	25.9	15.5	58.6
San Diego	8.6	22.6	68.8
Average imagery for SCB	23.2	14.1	62.7

approximately 30% of cloud-free area after a few days, compared to less than 20% of cloud-free area using AVHRR. The quality of MODIS images was poorest for the San Pedro area, which differed from the spatial patterns obtained with the other satellites.

3.2. Ship-based data

Ships were found to be capable of deployment for sampling approximately 70% of the time in the 10 days following rainstorms (Table 5). They were likely to be weathered out only about 10% of the time, with conditions being marginal for deployment on the remainder of the days. These numbers differed little among ships or regions.

Unlike the availability of satellite imagery, ship deployment success was generally high on the day of a storm, but declined

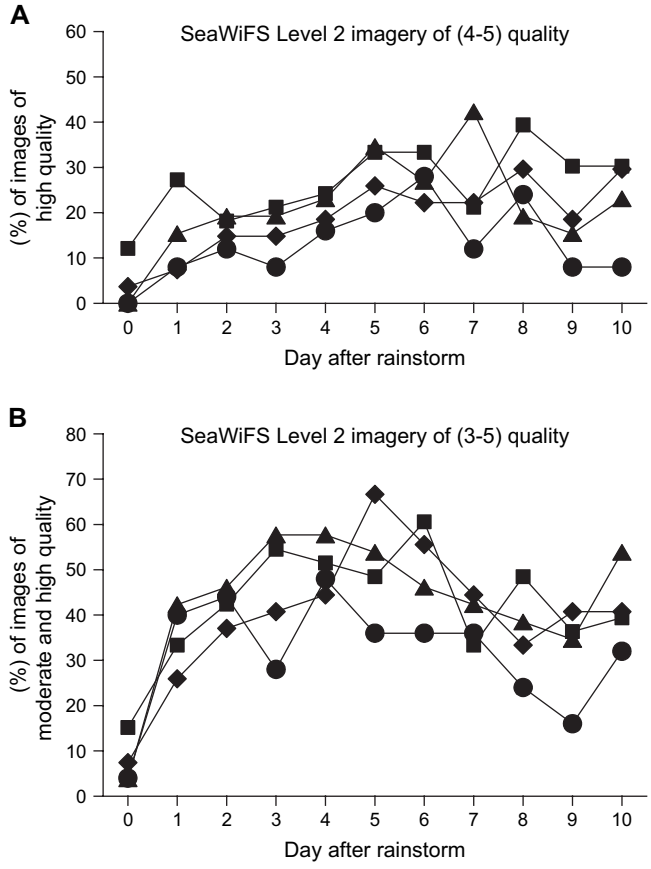

Fig. 2. Percentages of SeaWiFS imagery of high (A; grades 4–5) and moderate and high (B; grades 3–5) quality during the day of rainstorm and the next 10 days. Boxes – Ventura; diamonds – Santa Monica; triangles – San Pedro Shelf; circles – Orange County/San Diego.

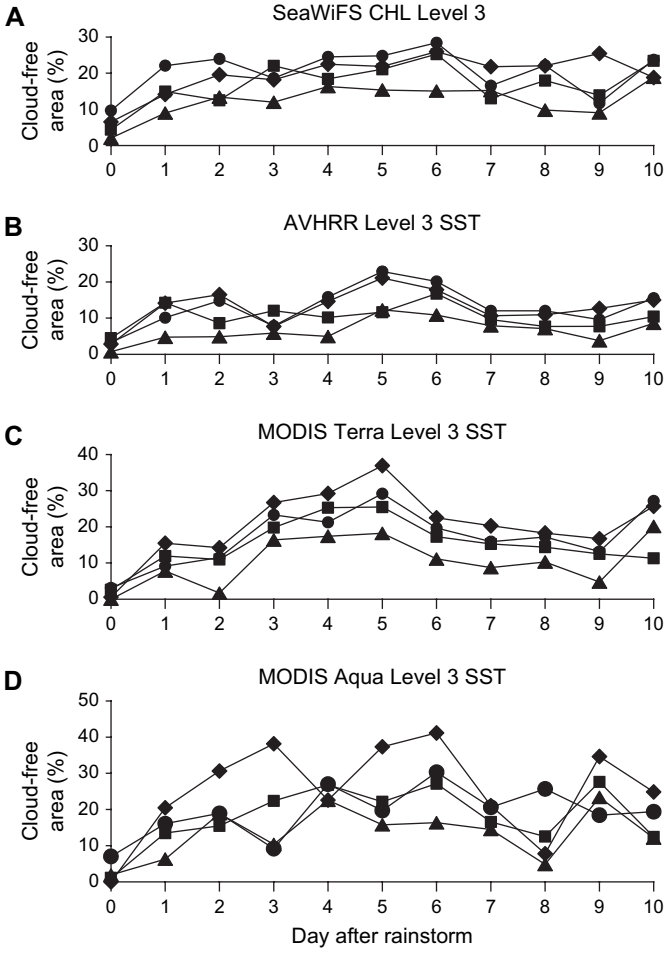

Fig. 3. Coverage of four coastal areas of southern California by Level 3 data of different satellite sensors. (A) SeaWiFS CHL; (B) AVHRR SST; (C) MODIS-Terra SST; (D) MODIS-Aqua SST. Boxes – Ventura; diamonds – Santa Monica; triangles – San Pedro Shelf; circles – Orange County/San Diego.

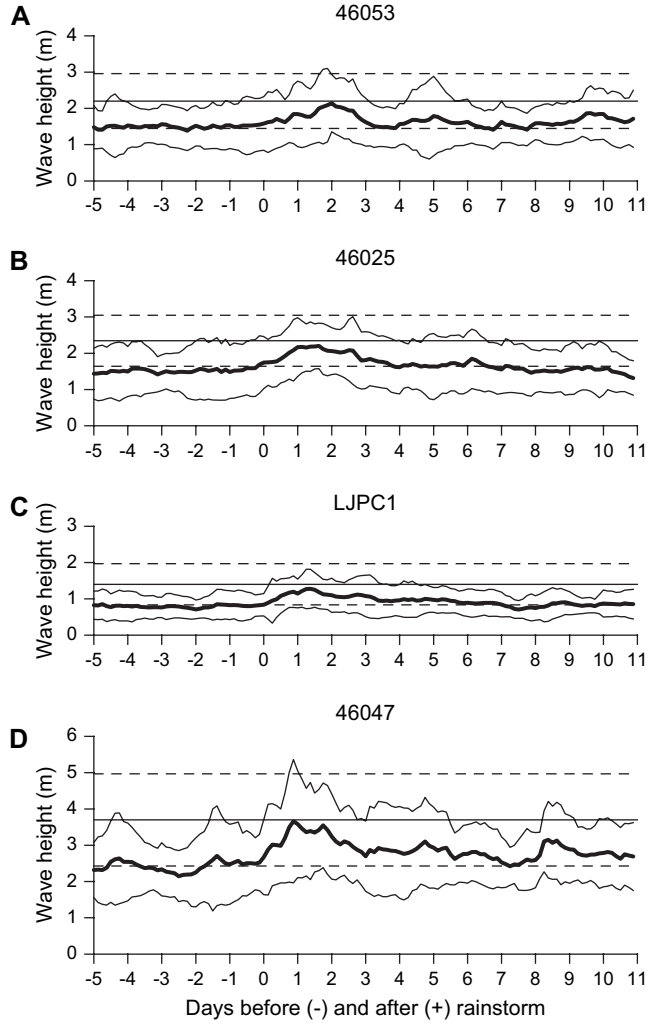

Fig. 4. Absolute wave height averaged for 3-h periods from 5 days before rainstorm to 10 days after rainstorm. Thick line indicates mean for each 3-h period, thin lines indicate mean ± standard deviation (SD). Horizontal lines indicate the values averaged for the days when the boat trips were weathered out (mean ± SD).

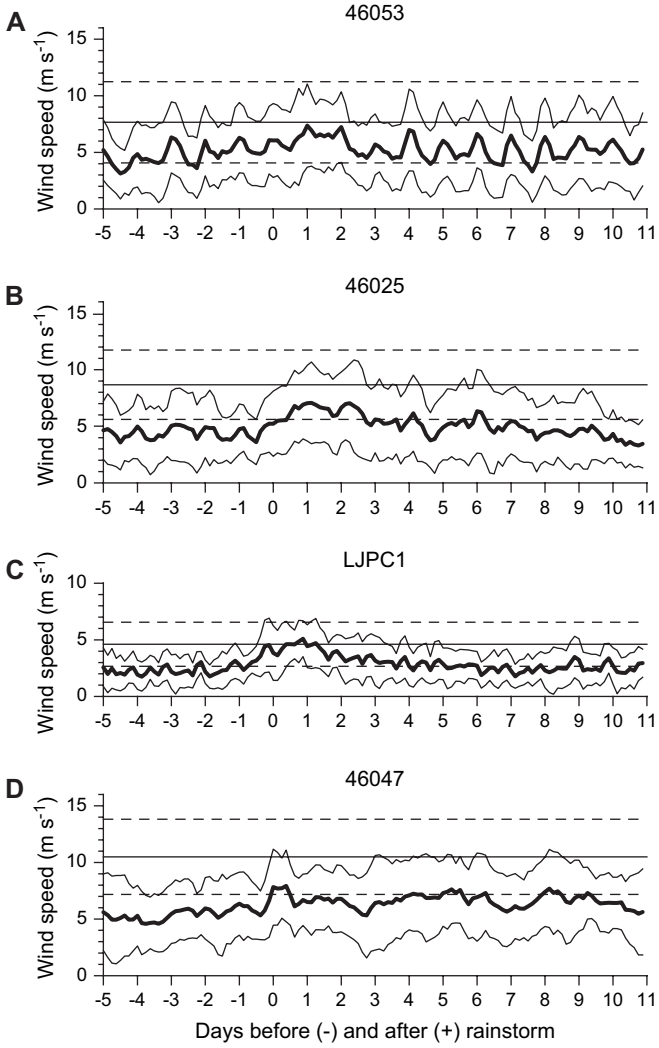

Fig. 5. Absolute wind speed averaged for 3-h periods from 5 days before rainstorm to 10 days after rainstorm. Thick line indicates mean for each 3-h period, thin lines indicate mean ± standard deviation (SD). Horizontal lines indicate the values averaged for the days when the boat trips were weathered out (mean ± SD).

over the next several days. This mostly resulted from wave height, which increased significantly at all six buoys in the 3 days after rainstorms (Fig. 4). Wind speed patterns were less consistent, with increases following rainstorms at the inshore buoy LJPC1 (Fig. 5C) and to a lesser extent at buoy 46025 in Santa Monica Bay (Fig. 5B). Similar changes were less evident at buoy 46053 in Santa Barbara Channel (Fig. 5A) and were almost absent in the central part of SCB (buoy 46047, Fig. 5D).

3.3. Concordance of ship deployment success and SeaWiFS imagery

The days for which the probability of successful ship deployment was lowest typically differed from the days for which the likelihood of obtaining usable satellite imagery was lowest (Table 6). Thus, for the 10 days following a storm, data from one of the tools were available 80% of the time. On the day of a storm, only ship-based data were typically available and for approximately 25% of the days neither method would have produced data (Fig. 6). By the fifth day following the storm, data were typically available using at least one of the methods for about 90% of the time.

4. Discussion

The plume parameters measured by satellite imagery and shipboard sampling differ and these methods should not be thought of as complete substitutes. Satellites detect a surface signature based on changes in ocean color (optical sensors) or sea surface roughness (SAR). In situ sampling provides direct quantitative measurements of additional parameters (e.g., chemical pollutants) and provides such information at multiple depths. The correlations between surface signatures and water quality characteristics are a means for transforming remotely sensed data into parameters of management interest, but the

Table 6
Joint probabilities for conditions being favorable for boat sampling and for obtaining informative satellite images in different areas of the Southern California Bight averaged for the 10 days starting from the day of rainstorm

Satellite imagery	Boat sampling conditions		
	Bad (%)	Moderate (%)	Good (%)
Ventura			
Bad	19.4	23.6	19.5
Moderate	1.5	5.6	1.6
Good	7.2	14.3	7.3
Santa Monica			
Bad	21.1	18.5	21.2
Moderate	2.3	4.9	2.4
Good	10.7	8.2	10.7
San Pedro			
Bad	20.6	17.5	20.5
Moderate	2.0	11.3	2.2
Good	8.2	9.3	8.4
San Diego			
Bad	19.1	30.5	19.2
Moderate	6.8	8.9	6.9
Good	2.6	3.2	2.8
Total for all four regions			
Bad	20.1	22.5	20.1
Moderate	3.1	7.7	3.3
Good	7.2	8.7	7.3

accuracy of such transformations in the nearshore zone has yet to be fully established (Muller-Karger et al., 2005).

The biggest advantage of satellite imagery is that it costs less and provides a more synoptic coverage of the plume pattern than in situ sampling. Unfortunately, the frequency of clear imagery from presently deployed satellites appears insufficient to serve as a primary means for assessing plume dynamics in the SCB. Only ~23% of SeaWiFS imagery provided enough information about plume patterns following rainstorms, when plumes are of greatest interest. Moreover, imagery was least available on days immediately following storms, when the plumes are evolving most rapidly.

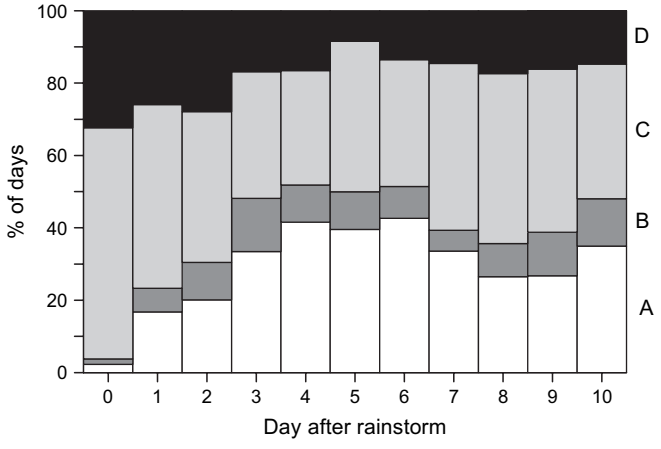

Fig. 6. Joint probabilities for conditions being favorable for boat sampling and for obtaining good satellite images in the Southern California Bight for the 10 days after a rainstorm. (A) "Moderate/Good" boat sampling and "Moderate/Good" SeaWiFS imagery; (B) "Bad" boat sampling and "Moderate/Good" SeaWiFS imagery; (C) "Moderate/Good" boat sampling and "Bad" SeaWiFS imagery; (D) "Bad" boat sampling and "Bad" SeaWiFS imagery.

Although satellite imagery may not be a substitute for ship-based sampling, it can provide a meaningful complement to ship-based measurements. While the likelihood of obtaining an informative satellite image is low during rainstorms, it dramatically improves during the days following a storm. Meteorological conditions in the SCB typically change after rainstorms to strong northwesterly winds (Nezlin and Stein, 2005), which blow out most clouds and make the coastal ocean more visible to satellites. At the same time, this strong wind condition creates problems for ships, hindering water sampling during the period when the size of a plume is at its maximum (Nezlin et al., 2005). Obtaining data during this period is especially important because this is when plumes begin to degenerate. Plume persistence in Santa Monica Bay, as estimated from salinity measurements, is about 3 days (Washburn et al., 2003), though a plume may persist as long as 5–7 days after strong rainstorms (Nezlin et al., 2005).

Of the satellite imagery examined, MODIS provided the best quality plume data. The cloud-detection algorithm of MODIS is based on a higher number of visible and infrared channels (total of 36 channels) than either AVHRR (5 channels) or SeaWiFS (8 channels). Moreover, some of these MODIS channels are available at higher spatial resolution (250 m and 500 m), compared to the 1 km spatial resolution of the other satellites. As a result, fewer pixels in MODIS images are subjected to cloud contamination. The number of cloud-free pixels was lowest for the AVHRR sensor and was comparable with global figures (10–20%) typical for AVHRR (McClain et al., 1985; Saunders and Kriebel, 1988; Martin, 2004).

MODIS has the additional advantage of being mounted on two satellites: *Terra*, which passes across the equator from north to south at ~10:30 local time, and *Aqua*, which passes the equator south to north at ~13:30 local time. These two daily passes result in a substantial increase in availability of imagery, especially during periods of partial cloud cover that typically follow rainstorms. Features covered by clouds in one image are often visible in the second taken only a few hours later. Combining images from the two MODIS satellites during the first day after rainstorm leads to almost 50% availability of clear coastal ocean area, compared with ~20% for each MODIS sensor alone (Fig. 7). As the number of earth-observing satellites increases, the reliability of satellite monitoring should increase proportionately.

The availability of usable imagery for assessing plume properties can also be improved by the development of algorithms that allow integration of information across satellite types. This would be easiest when combining images of a similar type and resolution, such as MODIS, SeaWiFS and AVHRR. However, there are other opportunities for synergy. For example, we did not include the GOES satellites in our analyses because this type of satellite's high geostationary orbit results in much lower resolution images that would not be very useful alone. However, the increased frequency of image

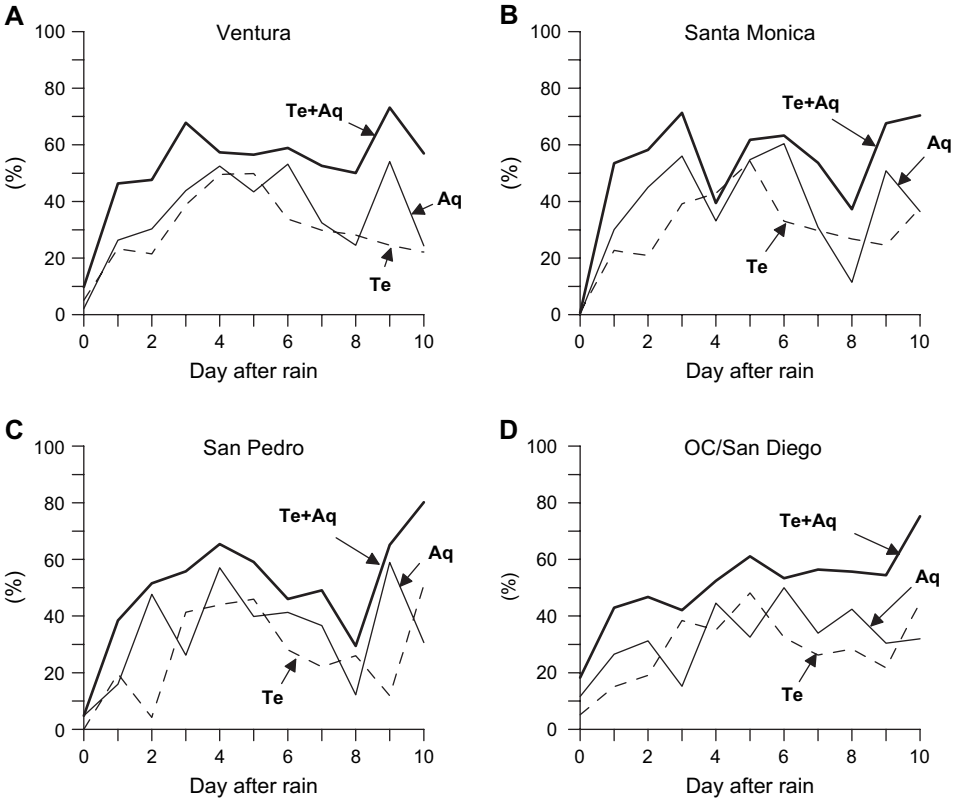

Fig. 7. Percent of cloud-free coastal ocean area in MODIS SST images for four regions of southern California during the day of rainstorm and the next 10 days. Dashed line is daytime MODIS-Terra (Te); thin solid line is daytime MODIS-Aqua (Aq); thick solid line is combined daily imagery of daytime MODIS-Terra and MODIS-Aqua (Te + Aq).

availability associated with geostationary orbit allows many opportunities each day to augment cloud-covered pixels in the higher resolution images available from other satellites. Additionally, the image quality of geostationary satellites might improve after the launch of the Hyperspectral Environmental Suite – Coastal Waters (HES-CW) sensor on GOES-R satellite, planned for 2012. This sensor will provide ocean color data at 300-m resolution every 3 h, and therefore, will be extremely useful in runoff plume monitoring. Similarly, we did not evaluate synthetic aperture radar (SAR), as this is a microwave sensor that measures sea surface roughness. While this is a more indirect measure than visible properties, SAR has been used to illustrate small-scale hydrographical phenomena like eddies (DiGiacomo and Holt, 2001) and freshwater plumes (Svejkovsky and Jones, 2001; DiGiacomo et al., 2004). Integrating microwave and optical sensors may present challenges, but microwaves are uninhibited by atmospheric conditions and can provide complementary information for every pixel when optical properties are partially obscured.

5. Conclusions

High-resolution satellite imagery is an important tool for studying coastal pollution, especially when it is used in combination with water samples collected after strong rainstorms. The advantages of satellite imagery over shipboard sampling are lower costs and a synoptic view of freshwater discharge plumes, but the availability of the data collected by modern satellites (e.g., SeaWiFS) is typically insufficient to completely describe plume dynamics. Local meteorological conditions, which are typically worse than normal during and immediately following rainstorms, significantly impact the availability of both satellite imagery and ship-based data collection: cloud cover produces obstacles for remote sensing and wind speed and wave height make collection of water samples from small ships problematic. The probability of obtaining scientific data is minimal on the day of a rainstorm and gradually increases during 5 days following a storm event, with the probability of obtaining satellite data increasing faster than the probability of in situ observations. The days after a storm for which satellite imagery and ship-based data were available often differed, making these two data sources complementary rather than redundant.

Recently designed MODIS satellite sensors provide better imagery of the southern California coastal zone due to better spectral, spatial and temporal resolution. In particular, two MODIS sensors collecting data twice a day significantly improve the quality of information regarding plume dynamics, especially during the first few days after rainstorms under partly cloudy conditions. We expect that the availability of satellite imagery will increase in the future with further development of satellite technology.

Acknowledgements

The authors would like to thank the SeaWiFS Project (Code 970.2) and the DAAC (Code 902) at the NASA GSFC for the production and distribution of the SeaWiFS data and images, respectively. MODIS data were acquired as part of the NASA's Earth Science Enterprise and were processed by the MODIS Adaptive Processing System (MODAPS), archived and distributed by the Goddard DAAC. We also thank the NASA JPL PODAAC for Pathfinder SST data (PODAAC product 216). We also thank the City of Los Angeles and the City of San Diego for access to their ship logs. Funding for this project was provided through the NOAA Coastal Services Center and we thank our project manager, Rebecca Smyth.

References

Ackerman, D., Weisberg, S.B., 2003. Relationship between rainfall and beach bacterial concentrations on Santa Monica Bay beaches. Journal of Water and Health 1, 85–89.

Ahn, J.H., Grant, S.B., Surbeck, C.Q., DiGiacomo, P.M., Nezlin, N.P., Jiang, S., 2005. Coastal water quality impact of stormwater runoff from an urban watershed in southern California. Environmental Science and Technology 39, 5940–5953.

Bay, S., Jones, B.H., Schiff, K., Washburn, L., 2003. Water quality impacts of stormwater discharges to Santa Monica Bay. Marine Environmental Research 56, 205–223.

Cracknell, A.P., 1997. The Advanced Very High Resolution Radiometer (AVHRR). Taylor & Francis, London, 534 pp.

DiGiacomo, P.M., Holt, B., 2001. Satellite observations of small coastal ocean eddies in the Southern California Bight. Journal of Geophysical Research 106, 22521–22543.

DiGiacomo, P.M., Washburn, L., Holt, B., Jones, B., 2004. Coastal pollution hazards in southern California observed by SAR imagery: stormwater plumes, wastewater plumes, and natural hydrocarbon seeps. Marine Pollution Bulletin 49, 1013–1024.

Isaaks, E.H., Srivastava, R.M., 1989. Applied Geostatistics. Oxford University Press, New York, 561 pp.

Kilpatrick, K.A., Podesta, G.P., Evans, R., 2001. Overview of the NOAA/NASA advanced very high resolution radiometer Pathfinder algorithm for sea surface temperature and associated matchup database. Journal of Geophysical Research 106, 9179–9197.

Martin, S., 2004. An Introduction to Ocean Remote Sensing. Cambridge University Press, Cambridge, 426 pp.

McClain, C.R., Feldman, G.C., Hooker, S.B., 2004. An overview of the SeaWiFS project and strategies for producing a climate research quality global ocean bio-optical time series. Deep-Sea Research II 51, 5–42.

McClain, E.P., Pichel, W.G., Walton, C.C., 1985. Comparative performance of AVHRR-based multichannel sea surface temperatures. Journal of Geophysical Research 90, 11587–11601.

Mertes, L.A.K., Warrick, J.A., 2001. Measuring flood output from 110 coastal watersheds in California with field measurements and SeaWiFS. Geology 29, 659–662.

Mertes, L.A.K., Hickman, M., Waltenberger, B., Bortman, A.L., Inlander, E., McKenzie, C., Dvorsky, J., 1998. Synoptic views of sediment plumes and coastal geography of the Santa Barbara Channel, California. Hydrological Processes 12, 967–979.

Monahan, E.C., Pybus, M.J., 1978. Colour, UV absorbance and salinity of the surface waters off the west coast of Ireland. Nature 274, 782–784.

Muller-Karger, F.E., Hu, C., Andrefouet, S., Varela, R., Thunell, R.C., 2005. The color of the coastal ocean and applications in the solution of research and management problems. In: Miller, R.L., Del Castillo, C.E., McKee, B.A. (Eds.), Remote Sensing of Coastal Aquatic Environments. Springer, Dordrecht, pp. 101–127.

Nezlin, N.P., DiGiacomo, P.M., 2005. Satellite ocean color observations of stormwater runoff plumes along the San Pedro Shelf (southern California) during 1997 to 2003. Continental Shelf Research 25, 1692–1711.

Nezlin, N.P., Stein, E.D., 2005. Spatial and temporal patterns of remotely-sensed and field-measured rainfall in southern California. Remote Sensing of Environment 96, 228–245.

Nezlin, N.P., DiGiacomo, P.M., Stein, E.D., Ackerman, D., 2005. Stormwater runoff plumes observed by SeaWiFS radiometer in the Southern California Bight. Remote Sensing of Environment 98, 494–510.

Noble, R.T., Weisberg, S.B., Leecaster, M.K., McGee, C.D., Dorsey, J.H., Vainik, P., Orozco-Borbon, V., 2003. Storm effects on regional beach water quality along the southern California shoreline. Journal of Water and Health 1, 23–31.

Otero, M.P., Siegel, D.A., 2004. Spatial and temporal characteristics of sediment plumes and phytoplankton blooms in the Santa Barbara Channel. Deep-Sea Research II 51, 1129–1149.

Reeves, R.L., Grant, S.B., Mrse, R.D., Copil Oancea, C.M., Sanders, B.F., Boehm, A.B., 2004. Scaling and management of fecal indicator bacteria in runoff from a coastal urban watershed in southern California. Environmental Science and Technology 38, 2637–2648.

Sathyendranath, S. (Ed.), 2000. Remote Sensing of Ocean Colour in Coastal and Other Optically-Complex Waters, vol. 3. IOCCG, Dartmouth, Canada, 140 pp.

Saunders, R.W., Kriebel, K.T., 1988. An improved method for detecting clear sky and cloudy radiances from AVHRR data. International Journal of Remote Sensing 9, 123–150.

Schiff, K.C., Bay, S., 2003. Impacts of stormwater discharges on the nearshore benthic environment of Santa Monica Bay. Marine Environmental Research 56, 225–243.

Siddorn, J.R., Bowers, D.G., Hoguane, A.M., 2001. Detecting the Zambezi River plume using observed optical properties. Marine Pollution Bulletin 42, 942–950.

Svejkovsky, J., Jones, B., 2001. Satellite imagery detects coastal stormwater and sewage runoff. EOS 82, 621–630.

Toole, D.A., Siegel, D.A., 2001. Modes and mechanisms of ocean color variability in the Santa Barbara Channel. Journal of Geophysical Research 106, 26985–27000.

Vasilkov, A.P., Burenkov, V.I., Ruddick, K.G., 1999. The spectral reflectance and transparency of river plume waters. International Journal of Remote Sensing 20, 2497–2508.

Warrick, J.A., Mertes, L.A.K., Washburn, L., Siegel, D.A., 2004a. Dispersal forcing of southern California river plumes, based on field and remote sensing observations. Geo-Marine Letters 24, 46–52.

Warrick, J.A., Mertes, L.A.K., Washburn, L., Siegel, D.A., 2004b. A conceptual model for river water and sediment dispersal in the Santa Barbara Channel, California. Continental Shelf Research 24, 2029–2043.

Washburn, L., McClure, K.A., Jones, B.H., Bay, S.M., 2003. Spatial scales and evolution of stormwater plumes in Santa Monica Bay. Marine Environmental Research 56, 103–125.